PERGAMON

International Journal of Heat and Mass Transfer 42 (1999) 1491–1499

International Journal of HEAT and MASS TRANSFER

Validation of an electronic anti-fouling technology in a single-tube heat exchanger

Y.I. Cho*, Byung-Gap Choi

Department of Mechanical Engineering and Mechanics, Drexel University, Philadelphia, PA 19104, U.S.A.

Received 3 February 1988; in revised form 5 June 1988

Abstract

The objective of the present study was to investigate the validity of an electronic anti-fouling (EAF) technology in the mitigation of precipitation fouling in a once-through flow system with a single-tube heat exchanger. Effects of flow velocity and water hardness on the effectiveness of the EAF technology were experimentally studied. The water hardness varied from 7.5 to 10 mol m^{-3} as $CaCO_3$. For both 7.5 and 10 mol m^{-3} solutions, the EAF treatment reduced fouling resistance by 20–38% at a flow velocity between 0.52 and 0.78 m s^{-1}. As the velocity decreased to 0.28 m s^{-1}, the EAF treatment was not helpful in reducing fouling. SEM photographs of scale produced from the 10 mol m^{-3} solution at 0.78 m s^{-1} indicated that calcium carbonate scales without the EAF treatment were needle-shaped aragonite, which is sticky, dense, and difficult to remove. Scales with the EAF treatment showed a cluster of elliptic shape crystals. Both the heat transfer test results and SEM photographs obtained in the present study support the validity of the EAF technology in mitigating precipitation fouling.

Nomenclature

A heat transfer surface area [m^2]
A cross sectional area vector [m^2]
B magnetic field strength vector [N A^{-1} m^{-1}]
d_O outside tube diameter [m]
D_H hydraulic diameter [m]
D_S inside shell diameter [m]
E induced electric field intensity vector [V m^{-1}]
Q heat transfer rate [W]
R_f fouling resistance [m^2 K W^{-1}]
s line vector along the circumferential direction [m]
t time [s]
$T_{c,in}$ inlet temperature of cold water [K]
$T_{c,out}$ outlet temperature of cold water [K]
ΔT_{LMTD} log-mean-temperature-difference [K]
U overall heat transfer coefficient based on outside tube diameter [W m^{-2} K^{-1}]
U_{clean} overall heat transfer coefficient at clean state [W m^{-2} K^{-1}]

1. Introduction

When hard water is heated (or cooled) in heat transfer equipment, scaling occurs. When scales deposit on a heat exchanger surface, it is traditionally called 'fouling'. The type of scale differs from industry to industry, depending on the mineral content of the available water. One of the most common forms of scale is calcium carbonate, $CaCO_3$, which is the subject of the present study.

Once scales build up on a heat transfer surface, at least two problems associated with scales occur. The first problem is the degradation in the performance of the heat transfer equipment. Due to the small thermal conductivity of scales, a thin coating of scales on the heat transfer surface will greatly reduce the overall heat transfer performance. The second problem is that a small change in tube diameter substantially decreases the flow rate or increases the pressure drop across the heat transfer equipment.

Various scale-inhibiting chemicals such as dispersing or chelating agents are used to prevent scales [1]. Ion exchange and reverse osmosis are also used to reduce water hardness, alkalinity, and silica level [1]. However, these methods are expensive at the industrial level, and require heavy maintenance for proper operation. Once

* Corresponding author. Tel.: 001 215 895 2425; fax: 001 215 895 1478; e-mail: ycho@coe.drexel.edu

0017–9310/98/$ - see front matter
PII: S0017–9310(98)00196–3

fouling occurs in a heat exchanger, scales are removed by using acid chemicals, which shorten the life of heat exchanger tubes, thus necessitating premature replacement. When acid cleaning is not desirable, scraping, hydro-blasting, sand blasting, metal or nylon brushing is used, operations which incur downtime and repair costs.

The objective of the present study was to conduct fouling experiments in a once-though flow system to examine whether an electronic anti-fouling technology mitigates precipitation fouling in a heat exchanger or not. Flow velocity and water hardness were varied to provide different fouling conditions, in which the performance of an electronic anti-fouling treatment was examined.

2. Operating principle of electronic anti-fouling technology

Figure 1 shows a schematic diagram of the operation of an electronic anti-fouling (EAF) device. A wire is wrapped around a feed pipe to a heat exchanger, forming a solenoid. The two ends of the wire are connected to the EAF control unit. The EAF unit produces a pulsing current to create time-varying magnetic fields inside the pipe. Subsequently, the time-varying magnetic field creates an induced electric field inside the pipe, a phenomenon which can be described by Faraday's law [2]:

$$\int \mathbf{E}\cdot\mathrm{d}\mathbf{s} = -\frac{\partial}{\partial t}\int \mathbf{B}\cdot\mathrm{d}\mathbf{A} \tag{1}$$

In order to maximize the induction, a pulsing current having a square-wave signal is used. The current and frequency of the square-wave signal used in the present study were 0.2 A and 500 Hz respectively. More detailed descriptions on the operating principle of the electronic anti-fouling device can be found elsewhere [3–7].

The induced electric field, which oscillates with time, provides molecular agitation to charged mineral ions such that dissolved mineral ions such as calcium and bicarbonate collide and precipitate with the help of impurities in water (e.g. iron oxide particles).

$$Ca^{2+} + 2HCO_3^- \rightarrow CaCO_3 + H_2CO_3 \tag{2}$$

As fluid temperature increases inside a heat exchanger, precipitated $CaCO_3$ particles and heat exchanger surface compete for dissolved mineral ions inside the heat exchanger. Since the combined surface area of the $CaCO_3$ particles can be greater than the surface area of the heat exchanger, the fouling at the heat exchanger surface can be mitigated or prevented.

The concept of introducing fine particles to reduce fouling is not new. Troup and Richardson [8], who reviewed both chemical and physical methods of water treatment used to prevent fouling in heat exchangers, reported that fouling could be reduced by simply feeding fine $CaCO_3$ particles or forming $Al(OH)_3$ particles in solution using aluminum electrodes across which an alternating current was passed.

It is of note that the precipitation of $CaCO_3$ particles by the electronic anti-fouling technology occurs in the presence of hard water. Hard water has excess dissolved mineral ions well above the saturation limit of each dissolved ion, and hence the water becomes unstable [9]. It is this supersaturated and unstable nature of hard water that causes 'severe' fouling in a heat exchanger in a time period of weeks or months. Of course, fouling also occurs with saturated water when it becomes supersaturated inside a heat exchanger. In this case, the fouling takes place slowly, i.e. over a period of years, and the use of

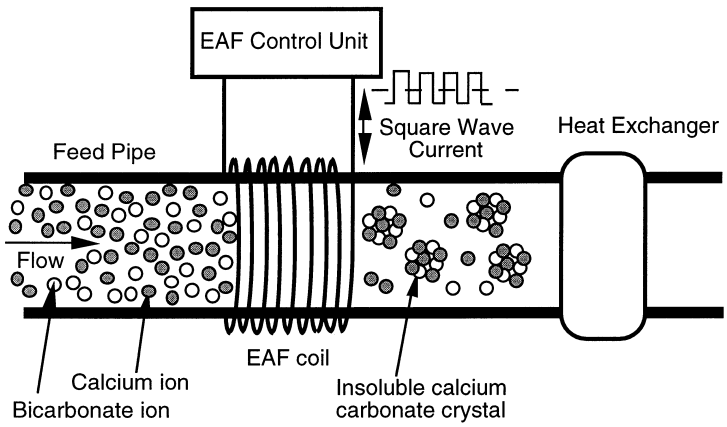

Fig. 1. Schematic diagram of the concept of electronic anti-fouling (EAF) technology. EAF control unit produces a solenoid-induced molecular agitation through Faraday's law and is installed in a feed pipe prior to heat exchanger.

either chemical or physical scale prevention method is often not justified from economical reasons.

3. Experimental method

Figure 2 schematically shows the test facility which consists of two reservoir tanks, two pumps, two flow meters, a static mixer, an electronic anti-fouling control unit, a solenoid coil, the main heat transfer test section made of a shell-and-tube heat exchanger, and a plate-and-frame heat exchanger.

Most previous fouling studies [10–15] were conducted using a recirculating flow system. The critical drawback of conducting a fouling test using a recirculating system is the continuous reduction of hardness during the test. Indeed, most fouling problems in the real world occur in a once-through flow system or in a circulating system where the hardness of cooling water does not vary with time. In order to create the best simulation of fouling problems occuring in the real world, the present study conducted fouling test in a once-through flow system.

The main heat transfer test section was made of two concentric copper tubes, which form a counter-flow heat exchanger. Two reducing unions were used at both the inlet and outlet of the heat exchanger for easy connection between the heat exchanger and connecting tubes. Hard (cold) water was pumped to the shell side whereas hot water moved through the tube side. Hence, scales were deposited on the shell side only. The inside shell diameter was $D_S = 0.01684$ m, whereas the tube outside diameter was $d_O = 0.01275$ m, rendering the hydraulic diameter $D_H = 0.00409$ m. The diameter of both the inlet and outlet connecting tubes was 0.0109 m. The axial length of the tube in the heat exchanger was 0.7 m.

Since the hardness of tap water available in Philadelphia is approximately 1.5 mol m^{-3} as $CaCO_3$, it is not suitable for fouling experiments. Note that 1 mol m^{-3} is equal to 100 mg L^{-1} for $CaCO_3$. Therefore, hard water in a range of 7.5 to 10 mol m^{-3} was prepared in a laboratory. For example, in order to prepare 10 mol m^{-3} $CaCO_3$ solution, calcium chloride ($CaCl_2$) of 444 g was dissolved in one tank containing 0.2 m^3 water, and sodium bicarbonate ($NaHCO_3$) of 672 g was dissolved in the other

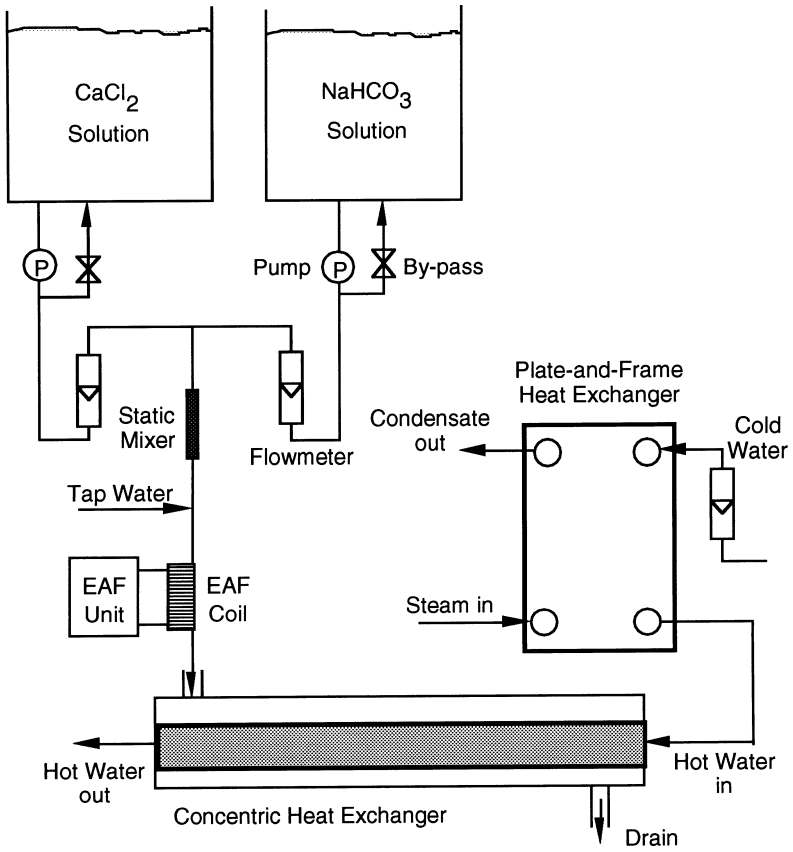

Fig. 2. Schematic diagram of a once-through flow system with a counter-flow single-tube heat exchanger. An EAF solenoid coil is located between pump and the inlet of the main heat transfer test section.

tank of the same size. The two solutions were pumped using two separate pumps, passed through flow meters, and later mixed using a static mixer as shown in Fig. 2. Table 1 gives values of alkalinity, electric conductivity, and pH of each concentration solution.

The inlet temperature of the hard water was maintained at 302 ± 0.5 K for all tests. Flow rates varied from 2.71×10^{-5} m^3 s^{-1} (0.43 U.S. gal min^{-1}) to 7.57×10^{-5} m^3 s^{-1} (1.2 U.S. gal min^{-1}), which resulted in the shell-side velocity of 0.28 and 0.78 m s^{-1}, respectively. The Reynolds numbers corresponding to 0.28 and 0.78 m s^{-1} were 1870 and 5020, respectively. It is of note that the viscosity and density of the hard water used in the Reynolds number calculation were evaluated at an average temperature of the hard water.

Thermocouples used in the present study were Omega model TMTSS-125G-6 (grounded copper–constantan T type). Calibration was carried out at 273 and 373 K, confirming the manufacturer's claim of the accuracy of ± 0.1 K. The temperature of the hot stream entering the tube side varied from 355 to 367 ± 1.0 K. To produce hot water continuously, a plate-and-frame heat exchanger was used, where high pressure steam provided by the Philadelphia city steam network was used. Flow meters were also calibrated over a range of 6.3×10^{-6} to 6.3×10^{-5} m^3 s^{-1} by measuring the weight of water accumulated over time, and the calibration results were reported elsewhere [16].

The overall heat transfer coefficient, U, was calculated as a function of time using the log-mean-temperature-difference (LMTD) [17], which was obtained from the four temperatures measured at both the inlet and outlet of cold and hot streams. Fouling resistance, R, was calculated using the usual definition [18].

$$Q = UA\Delta T_{\mathrm{LMTD}} = \dot{m}_{\mathrm{c}} C_{\mathrm{p}} (T_{\mathrm{c,out}} - T_{\mathrm{c,in}}) \tag{3}$$

$$U = \frac{\dot{m}_{\mathrm{c}} C_{\mathrm{p}} (T_{\mathrm{c,out}} - T_{\mathrm{c,in}})}{A\Delta T_{\mathrm{LMTD}}} \tag{4}$$

and

$$R_{\mathrm{f}} = \frac{1}{U(t)} - \frac{1}{U_{\mathrm{clean}}} \tag{5}$$

where U_{clean} is the overall heat transfer coefficient corresponding to the clean state, i.e. at $t = 0$. The U_{clean} average values for 0.28, 0.52, 0.65 and 0.78 m s^{-1} cases were 2460, 2116, 3445 and 4130 W m^{-2} K^{-1}, respectively.

The errors estimated from the uncertainty analysis for Q, U, R_{f} and A (heat transfer surface area) were 2.5%, 2.8%, 7.7%, and 1.1%, respectively. During the course of the present fouling experiment, it was discovered that the accuracy of the outlet temperature reading could be significantly affected by the scaling of the thermocouple probe itself [19]. Therefore, the thermocouple measuring the outlet temperature of the cold water was cleaned every time before each temperature measurement. It is speculated that much of the previous fouling data in the literature might have been seriously affected by the probe fouling because the thermocouple fouling could easily cause a temperature measurement error by several degrees [19].

4. Results and discussion

Figure 3 represents variation in fouling resistance as a function of time at a flow velocity of 0.78 m s^{-1} (1.2 U.S. gal min^{-1}) and a concentration of 10 mol m^{-3} with and without electronic anti-fouling (EAF) device. The hot water inlet temperature was 367 K for both cases, and the flow velocity of hot water was 2.23 m s^{-1} (3.3 U.S. gal min^{-1}). The fouling resistance for both cases, as manifested by the slopes in Fig. 3, increased linearly with time.

From the slope of the curve of R_{f} vs time in Fig. 3, the fouling rate without the EAF device was calculated as 1.45×10^{-6} m^2 K J^{-1}, whereas the value with the EAF device was 1.15×10^{-6} m^2 K J^{-1}. At the end of 86 min of operation, the fouling resistance without the EAF device was 1.30×10^{-4} m^2 K W^{-1}, whereas it was 1.05×10^{-4} m^2 K W^{-1} with the EAF device, a 20% drop.

It was hypothesized that the EAF treatment produced $CaCO_3$ particles, reducing the concentration of calcium ions in bulk solution and subsequently the scale deposit rate. In order to examine this hypothesis, a scanning electron microscope (SEM) was used to visualize crystal structures of scales. SEM photographs given in Figs. 4(a) and 4(b) were obtained from scaled tubes produced at a

Table 1
Values of alkalinity, electric conductivity, and pH of each concentration solution. Also shown are the amounts of calcium chloride ($CaCl_2$) and sodium bicarbonate ($NaHCO_3$) required for one liter of 7.5 and 10 mol m^{-3} solution

Concentration (mol m^{-3})	$CaCl_2$ (mol)	$NaHCO_3$ (mol)	Alkalinity (mg l^{-1})	Conductivity (μS cm^{-1})	pH
7.5	0.0075	0.015	760–810	3060–3190	7.88–8.10
10	0.01	0.02	980–1040	3860–3950	7.81–8.05

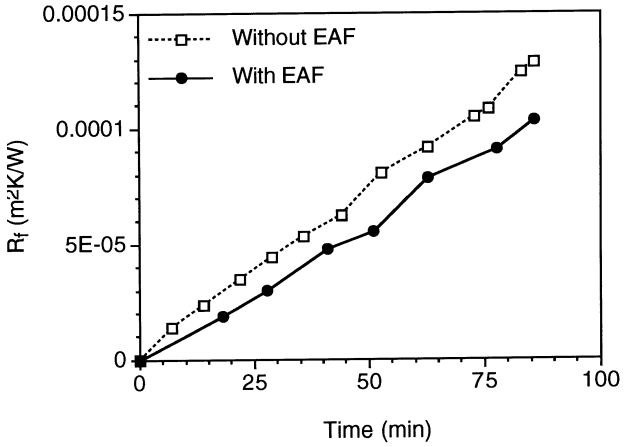

Fig. 3. Fouling resistances vs time for two different cases: without and with electronic anti-fouling (EAF) device. Concentration of test solution = 10 mol m^{-3}; cold water flow velocity = 0.78 m s^{-1}; hot water flow velocity = 2.23 m s^{-1}; hot water inlet temperature = 367 K.

flow velocity of 0.78 m s^{-1} and a concentration of 10 mol m^{-3} without and with EAF device, respectively.

Scale specimen for SEM was prepared with a utility knife by scraping small amounts of scales from the outlet region of each scaled tube. SEM photographs of scales produced without the EAF device (Fig. 4(a)) revealed that $CaCO_3$ scales were needle-shaped aragonite [20], whose dimensions were approximately 25 $\mu m \times 2$ μm. Aragonite is a dangerous form of calcium carbonate scale, which is crystallized at a temperature above 308 K [20]. It is sticky, dense, and difficult to remove. The long-needle shaped crystals confirm that the precipitation reaction occurred on the heat transfer surface without the EAF device.

In contrast, the scales produced with the EAF device (Fig. 4(b)) depicted a very different structure from the one produced without the EAF device. The scales produced with the EAF device were a cluster of small elliptic shape particles (e.g. 10 $\mu m \times 3$ μm) with no particular orientation, suggesting that many fine particles were formed in bulk solution, attached to the heat transfer surface, and then grew in size through precipitation reaction.

The SEM photographs in Fig. 4 support the hypothesis of the EAF technology, which is to convert dissolved mineral ions into crystals in a bulk solution, thus reducing both the diffusion of dissolved ions to the heat transfer surface and subsequent precipitation reaction on the heat transfer surface. As a result, the production of aragonite type calcium carbonate is prevented. Calcium carbonate crystals formed with the EAF device appeared to be loosely connected. In other words, the scales formed with the EAF device may be removed at a small flow velocity (e.g. 1 m s^{-1}), whereas the scales formed without the EAF device may not be removed even at a large flow velocity (e.g. 5 m s^{-1}).

Figure 5 represents variation in fouling resistance as a function of time at a flow velocity of 0.52 m s^{-1} and a concentration of 10 mol m^{-3} with and without the EAF device. The hot water inlet temperature was maintained at 361 K for both cases, and the flow velocity of hot water was 0.74 m s^{-1}. In spite of a reduced flow velocity of cold water (i.e. 0.52 m s^{-1}), the fouling resistance leveled off after approximately 90 min of operation, reaching asymptotic fouling resistances of 7.83×10^{-5} m^2 K W^{-1} and 6.03×10^{-5} m^2 K W^{-1} for the cases without and with the EAF device, respectively. The asymptotic fouling resistance obtained with the EAF device was 23% less than that without the EAF device.

Figure 6 shows variation in fouling resistance as a function of operating time at a cold water flow velocity of 0.28 m s^{-1} and a concentration of 10 mol m^{-3} with and without EAF device. The hot water inlet temperature was 367 K for both cases, and the flow velocity of hot water was 2.23 m s^{-1}—a severe fouling condition. At the end of 240 min of operation, the fouling resistance obtained with the EAF device was almost identical to the one obtained without the device. The EAF treatment at this reduced flow velocity was found to be not useful in mitigating fouling.

In order to understand why the EAF treatment did not reduce fouling under these severe fouling conditions, one can examine the fouling curve in Fig. 6. Initial fouling rate without the EAF device was greater than that with the EAF device (i.e. see the slope of the fouling curves at $t = 0$). Hence, more scales deposit on tube surface without the EAF device, reducing scale surface temperature. Subsequently, less scales deposit due to the decrease in the surface temperature, as indicated by arrow 'A' in Fig. 6. On the other hand, less scales deposit initially with the EAF device. Subsequently, the heat transfer surface maintains the initial high temperature, and fouling con-

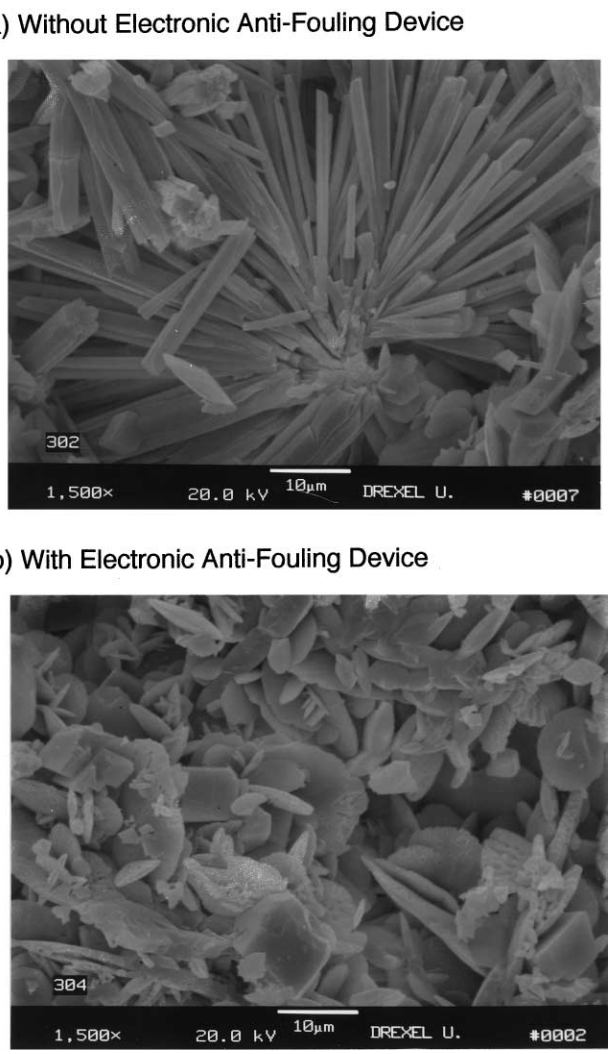

Fig. 4. Photographs taken using a scanning electron microscope with scale specimen from scaled tubes produced at a flow velocity of 0.78 m s^{-1} and a concentration of 10 mol m^{-3} (a) without electronic anti-fouling device and (b) with EAF device. Magnification = 1500×.

tinues to progress as indicated by arrow 'B' in Fig. 6. As enough scales deposit on the tube surface, the surface temperature drops eventually, resulting in the same asymptotic fouling resistance as the one without the EAF device.

Figure 7 presents variation in fouling resistance as a function of time at a flow velocity of 0.78 m s^{-1} and a concentration of 7.5 mol m^{-3} with and without the EAF device. The hot water inlet temperature was 367 K for both cases, and the flow velocity of hot water was 2.23 m s^{-1}. At the end of 89 minutes of operation, the fouling resistance without the EAF device was 5.09×10^{-5} m^2 K W^{-1}, whereas the value with the EAF device was 3.78×10^{-5} m^2 K W^{-1}, a 26% drop. Compared with the results given in Fig. 3, the percentage drop in the fouling resistance due to the EAF device was greater for the 7.5 mol m^{-3} solution than for the 10 mol m^{-3} solution, suggesting that as a fouling condition becomes less severe the benefit of the EAF treatment becomes larger.

In order to verify this suggestion, the inlet temperature of hot water was reduced from 367 K to 355 K, and the corresponding results obtained with and without the EAF device are shown in Fig. 8. The flow velocities of cold and hot water were 0.65 and 2.23 m s^{-1}, respectively. At the end of 105 min of operation, the fouling resistance without the EAF device was 5.25×10^{-5} m^2 K W^{-1}, whereas the value with the EAF device was 3.26×10^{-5} m^2 K W^{-1}, a 38% drop. As the hardness of cold water decreased from 10 to 7.5 mol m^{-3}, the percentage drop in the fouling resistance due to the EAF device increased from 20 to 38%. Of note is that the hardness of cooling tower water is usually maintained at an electric con-

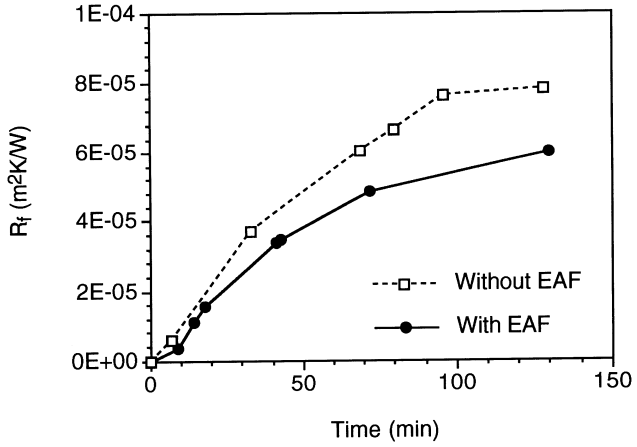

Fig. 5. Fouling resistances vs time for two different cases: without and with electronic anti-fouling (EAF) device. Concentration of test solution = 10 mol m^{-3}; cold water flow velocity = 0.52 m s^{-1}; hot water flow velocity = 0.74 m s^{-1}; hot water inlet temperature = 361 K.

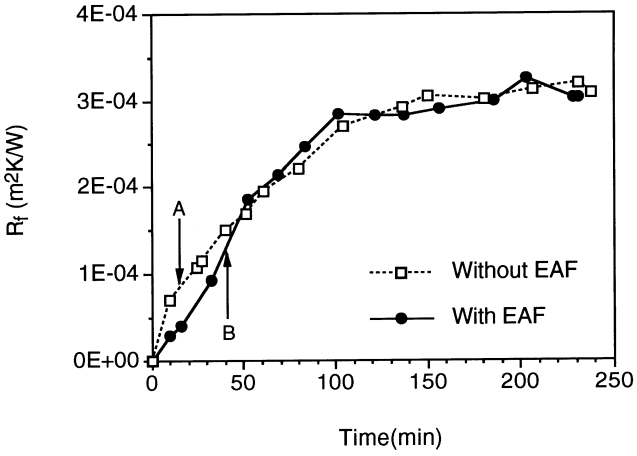

Fig. 6. Fouling resistances vs time for two different cases: without and with electronic anti-fouling (EAF) device. Concentration of test solution = 10 mol m^{-3}; cold water flow velocity = 0.28 m s^{-1}; hot water flow velocity = 2.23 m s^{-1}; hot water inlet temperature = 367 K.

ductivity between 1200 and 1500 μS cm^{-1}, which is equivalent to a hardness of approximately 4.5–5.0 mol m^{-3}. Hence, the EAF treatment should reduce the fouling resistance in a heat exchanger used in any cooling tower system at least 40%.

Figure 8 also shows a peculiar fouling behavior during the first 20 min of operation for both cases with and without the EAF device. As soon as tests started, the fouling resistance became negative for both cases, indicating that the overall heat transfer coefficient, U, increased from that of the clean state. This peculiar phenomenon has not been uncommon [18]. This can be explained as follows: the nascent fouling deposit produces a roughened heat transfer surface. As the surface becomes rough, the convective heat transfer coefficient increases through better mixing and breaking the laminar sublayer at the wall. Hence, the overall heat transfer coefficient initially improved, resulting in negative fouling resistances. As fouling deposits continue, the fouling layer acts as a thermal insulator, decreasing the overall heat transfer coefficient. The fouling resistance begins to increase and becomes positive at $t = 13$ min without the EAF device and at $t = 23$ min with the EAF device. The trend of the fouling resistance having negative values initially must have occurred for other tests shown in this paper. However, it is speculated that the period of the heat transfer improvement was too brief to observe.

It is of note that one of the problems of conducting fouling experiments in an actual heat exchanger is lack of knowledge of the continuously changing deposit–fluid

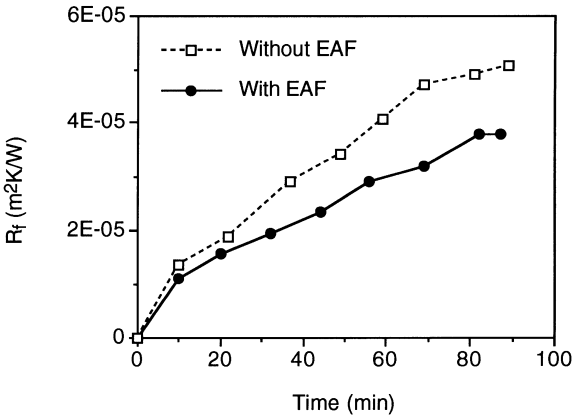

Fig. 7. Fouling resistances vs time for two different cases: without and with electronic anti-fouling (EAF) device. Concentration of test solution = 7.5 mol m^{-3}; cold water flow velocity = 0.78 m s^{-1}; hot water flow velocity = 2.23 m s^{-1}; hot water inlet temperature = 367 K.

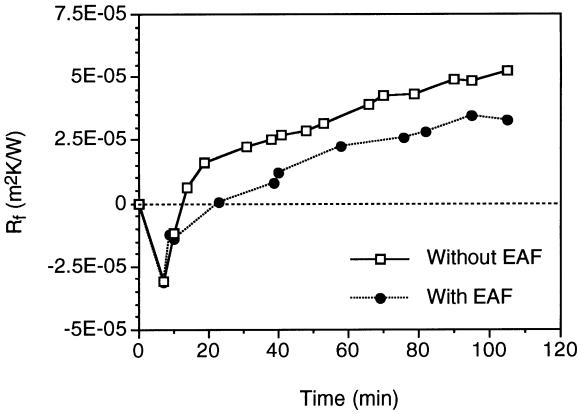

Fig. 8. Fouling resistances vs time for two different cases: without and with electronic anti-fouling (EAF) device. Concentration of test solution = 7.5 mol m^{-3}; cold water flow velocity = 0.65 m s^{-1}; hot water flow velocity = 2.23 m s^{-1}; hot water inlet temperature = 355 K.

interface temperature, which is one of the most important parameters in scaling analysis. This problem could have been overcome by using constant heat flux electric heating, which would have given a constant local deposit–fluid interface temperature that is equal to the initial measurable wall-surface temperature. Since actual heat exchangers do not use constant heat flux heating, this condition is usually not achieved in practice. Alternatively, one can analytically estimate the deposit-fluid interface temperature as a function of time using the NTU method [17] and a fouling modeling, a procedure which is summarized in Choi [16].

5. Conclusions

The present study was conducted in order to investigate the validity of electronic anti-fouling (EAF) technology, which was considered as a means to control new precipitation fouling in a heat exchanger. Fouling tests were carried out in a counter-flow shell-and-tube heat exchanger, and the fouling resistances obtained without the EAF device were compared with those obtained with the EAF device for two different water hardness (7.5 and 10 mol m^{-3}) and four different flow velocities (0.28, 0.52, 0.65, and 0.78 m s^{-1}).

Scanning electron microscope (SEM) photographs of scale produced without the EAF device revealed needle-shaped aragonite (i.e. sticky, dense, and difficult to remove), whereas the scale obtained with the EAF device produced a cluster of loosely-connected small elliptic shape particles (i.e. easier to remove than needle-shaped aragonite).

For the 10 mol m^{-3} solution at a velocity of 0.78 m s^{-1}, the fouling resistance with the EAF device was 20% smaller than that without it. As the hardness of water decreased from 10 to 7.5 mol m^{-3}, and the inlet temperature of hot water decreased from 367 to 355 K, the percentage drop in the fouling resistance due to the EAF device increased from 20 to 38%. However, at a reduced flow velocity at 0.28 m s^{-1} or less, the EAF treatment was not helpful in the mitigation of fouling.

Although the present paper uses calcium carbonate as an example of the mineral scales, the electronic anti-fouling treatment is not limited to the calcium carbonate scale. This is because the EAF treatment utilizes the electrical charges of dissolved ions to foster collision and precipitation into insoluble crystals.

References

[1] G. Tchobanoglous, F. Burton, Wastewater Engineering, Treatment, Disposal and Reuse, 3rd Ed. New York: McGraw-Hill, 1991.
[2] R.A. Serway, Physics for Scientists and Engineers, 3rd ed. Philadelphia, PA: Saunders College Publishing, 874–891, 1990.
[3] C.F. Fan, A study of electronic descaling technology to control precipitation fouling, Ph.D. thesis, Philadelphia, PA: Drexel University, 1997.
[4] C.F. Fan, Y.I. Cho, Microscopic observation of calcium carbonate particles: validation of an electronic anti-fouling technology, Int. Comm. Heat Mass Transfer 24 (1997) 757–770.
[5] C.F. Fan, Y.I. Cho, A new electronic anti-fouling method to control fouling, ASME Proceeding of the 32nd National Heat Transfer Conference HTD-Vol. 350 (12), Baltimore, Maryland, 1997, pp. 183–188.
[6] Y.I. Cho, C.F. Fan, B.G. Choi, Theory of electronic anti-

fouling technology to control precipitation fouling in heat exchangers, Int. Comm. Heat Mass Transfer 24 (1997) 747–756.
[7] Y.I. Cho, B.G. Choi, B.J. Drazner, Use of electronic descaling technology to control precipitation fouling in plate-and-frame heat exchanger. In Shah RK, editor, Compact Heat Exchangers for the Process Industries. New York, Begell House; 1997, pp. 267–273.
[8] D.H. Troup, J.A. Richardson, Scale nucleation on a heat transfer surface and its prevention, Chem. Eng. Comm. 2 (1978) 167–180.
[9] V.I. Snoeyink, D. Jenkins, Water Chemistry, Wiley, 1982.
[10] D. Hasson, M. Avriel, W. Resnick, T. Roseman, S. Windreich, Mechanism of calcium carbonate scale deposition on heat transfer surfaces, Int. Eng. Chem. Fund. 7 (1968) 59–65.
[11] R. Sheikholeslami, A.P. Watkinson, Scaling of plain and externally finned heat exchanger tubes, J. Heat Transfer 108 (1986) 147–152.
[12] A.P. Watkinson, O. Martinez, Scaling of heat exchanger tubes by calcium carbonate, J. Heat Transfer 97 (1975) 504–508.
[13] A.P. Watkinson, Water quality effects on fouling from hard waters. In Taborek J, et al, editors, Heat Exchangers—Theory and Practice. Hemisphere, 1983, pp. 853–861.
[14] N. Andritsos, M. Kontopoulou, A.J. Karabelas, Calcium carbonate deposit formation under isothermal conditions, Can. J. Chem. Eng. 74 (1996) 911–919.
[15] T.J. Rabas, J. Tarborek, Heat-rate improvements obtained by retubing condensers with new, enhanced tube types, J. Enhanced Heat Transfer 3 (1996) 83–94.
[16] B.G. Choi, A study of fouling control in heat exchangers with electronic anti-fouling technology, Ph.D. thesis, Drexel University, Philadelphia, PA, 1998.
[17] F.P. Incropera, D.P. DeWitt, Fundamentals of Heat and Mass Transfer, 4th ed. New York: Wiley, 1996.
[18] B. Bansal, Müller-Steinhagen, Crystallization fouling in plate heat exchangers, J. Heat Transfer 115 (1993) 584–591.
[19] Y.I. Cho, B.G. Choi, Effect of fouling on temperature measurements error and a solution, J. Heat Transfer 120 (1998) 525–528.
[20] J.C. Cowan, D.J. Weintritt, Water-Formed Scale Deposits. Houston, TX: Gulf Publishing Company, 1976.